Digest 2014, December 2014, 1733-1756

Dynamic Behavior of an Isolated Bridge Pier under Earthquake Effects for Different Soil layers and Support Conditions†

Fevzi SARITAŞ*
Zeki HASGÜR**

ABSTRACT

An isolated bridge pier having rubber bearings is modeled by finite element technique and dynamic responses under effects of earthquake accelerations are obtained by linear solution methods in time and frequency domain; the results are evaluated by probabilistic distributions. For this purpose, stationary accelerations characterized by Kanai-Tajimi power spectrum are simulated for different soil types and twenty nonstationary records in each soil group are obtained by modulating the amplitudes in harmony with Erzincan NS 1992 component. The pier responses and deck displacements are obtained in time domain for different support and soil conditions by using simulated horizontal and vertical accelerations. Furthermore, variances of the responses are obtained in frequency domain by assuming stationary stochastic behavior and by using power density and cross-power spectra of the applied simultaneous motions. The results are evaluated by those of the time domain solutions and peak responses and variations of peak response factors are determined. For dynamic peak responses, the response quantities corresponding to exceedance probabilities of 2%, 10% and 50% (median) are predicted depending upon soil types by use Rayleigh distribution model.

***Keywords**: Peak responses, rubber, Kanai-Tajimi, nonstationary, stochastic.*

1. INTRODUCTION

The most important function of bridges and viaducts allowing the passages of river and valley in road and railway transportations is to provide safety with limited damages without collapse and this case plays a great role in engineering designs for a probable earthquake motion. When damages occurred in bridge piers are examined, besides the pier stiffness it is seen that the ground conditions of soil and types of supports affect significantly the behavior of such structures. Differentiations in ground conditions cause significant changes in the seismic behavior of bridges having high piers and larger displacements can occur by softening uniform soil structure [1]. To reduce the amplification effects on the structural responses, drilling down to level of a suitable ground

* Pamukkale University, Denizli, Turkey - fsaritas@pau.edu.tr
** Istanbul Technical University, İstanbul, Turkey - hasgur@itu.edu.tr
† Published in Teknik Dergi Vol. 25, No. 2 April 2014, pp: 6699-6723

formation and also constructing the proper deep foundation may be needed for high piers. In the present case, the impacts of different soils inhabited piers between large spans are intended to be low on the behavior when such measures are taken. On the other hand, variations in pier heights may lead to increase in internal forces and displacements especially when the vibration frequency of bridge structure is in the vicinity of the dominant frequency of ground motion [2]. Furthermore, the flexibility of soil site is able to influence significantly the behavior of the rigid superstructure for the seismic isolated bridges and therefore the maximum response quantities can greatly vary [3]. Dicleli ve Karalar [4] has showed that the optimum values of mechanical properties of isolators represented by characteristic strength and post-elastic stiffness are highly dependent on the frequency content of ground motion and therefore on the soil conditions.

Dynamic behavior of a bridge subjected to earthquake effects can be determined by either deterministic methods in time-domain and or frequency domain methods based on random vibration theory known as stochastic analysis. Under the horizontal and vertical acceleration components, some researchers [5,6] analyzed the dynamic behavior of reinforced concrete highway bridges in a deterministic way by using the finite element method. Important information about the realistic behavior of bridges can be obtained by the stochastic technique considering inherent randomness in ground motion. In stochastic analysis of bridges and piers, nonstationary ground motions are defined by power spectrum based on filtered white noise model and by using time varying envelope functions for amplitudes. Output process (structural responses) are obtained depending on input process by means of frequency behavior function. A linear stochastic analysis of the seismic isolated pier taking into account stationary Gauss process and Kanai-Tajimi model for white noise has shown that the variations in responses are almost independent from the spectral content of the earthquake motion [7]. Jangid [8] examined the maximum responses of the bridges with the assumption of the elastic behavior for the piers under effect of nonstationary ground motions. In this study, equivalent optimum yield strength of the elastomeric bearing was determined by linearized stochastic methods. By assuming linear behavior for piers and superstructure, the maximum responses derived from the analyses with the adoption of different elastomeric bearings and sliding bearing systems were found to increase by the flexibility of the pier and superstructure [9]. In random vibration analysis performed by white noise model for a bridge pier designated as a cantilever beam with rubber bearing, it was found that the behavior of the first two modes get close to the rigid body motion as the bearing stiffness decreases [10]. Bridge pier with symmetric cantilevers having four degrees of freedom (DOF) subjected to horizontal and vertical acceleration components was studied and the stochastic behavior was derived in frequency domain in terms of base response variances [11]. There have been also different stochastic researches in bridge behavior which is taken into account by nonlinear wave-propagations of motion with local soil conditions [12]. For a long-span suspended bridge system exposed to earthquake effects handled by Kanai-Tajimi model with white noise spectrum, structural responses were obtained with stochastic analyses and it was shown that the method yielded applicable results [13]. Spectrum and frequency domain analyses with various bearing vibrations for a bridge exposed to stationary motions showed that structural responses are able to reach quite large values in the case of a soft site [14]. Time-dependent maximum responses under horizontal seismic effects also can be determined by using nonstationary

random processes considering together the semi-dynamic and the full integration method [15].

On the other hand, the maximum response factors ($r=[E(x_{max})]/RMS$) expressing the peak response quantities in a vibration motion are computed by the ratio between expected mean value ($[E(x_{max})]$) and root mean square value (RMS). This ratio is not constant and it takes a different value even for an acceleration record measured in another device in the same region. In obtaining peak response factors, the models suggested by Vanmarcke [16] and Davenport [17] have been widely used so far. Vanmarcke model contains constant power spectrum intensity of ground motion (So), damping and natural frequency parameters of the structure together with spectral moments of behavior. In this model, the effects of structural characteristics are low and very close values for peak response factors are obtained even for different systems.

In this study, a pier system with rubber bearing in a present bridge built on highway is analyzed to investigate the dynamic behavior effects of local soil conditions and the support type of the superstructure. The sizes of rubber bearings containing a lead core, box girder and pier cross-section are selected in general terms for the considered bridge system. The bridge symmetric-pier having box girder and double cantilever beam is modeled by finite elements and stochastic behavior is determined under the influences of nonstationary random ground motions by means of statistical terms such as mean and variance. For use in dynamic analysis, 20 nonstationary earthquake records are simulated for each of the different soil types through the Kanai-Tajimi filter functions and a time-dependent envelope functions. Both generating the artificial ground motions and obtaining the linear stochastic behavior of the system are realized by a developed computer algortihm. The usage of the method is demonstrated by the implementation of stochastic dynamic analysis over the system and the behavior influences of some characteristics (linear and nonlinear rubber bearing model, supporting types of the superstructure) are displayed depending upon soil site type. The maximum response quantities obtained in the frequency domain are compared with the solutions in time domain and it is shown that the results are in compatible relationship. In addition, the mean peak responses are determined by calculating the peak response factors for each soil type. On the other hand, the probability distribution functions and exceedance probabilitiy functions of maximum responses are obtained and shown in the graphs for different soil conditions. Advanced probabilistic analysis such as structural reliability or risk assessment that can be used in the design process may be performed by obtained the statistical values and probability functions.

2. ARTIFICIAL EARTHQUAKE RECORDS FOR DIFFERENT SOIL CONDITIONS

2.1. Kanai-Tajimi Model

Acceleration values ($\ddot{v}_k(t)$) of seismic waves that occur in bedrock till reaching the earth surface ($\ddot{v}_g(t)$) (Figure 1- schematized) are undergone large changes ($\ddot{v}_f(t)$) due to reflections and refractions in intermediary medium depending on elastic and damping properties of the soil site. The soil medium inhabited by piers considerably differentiate the frequency content of ground motion and in some instances it is observed that the soil

medium is able to increase seismic demand forces and cause significant damages [18]. Time dependent earthquake motions and their random character can be considered by stochastic models to represent variations in amplitudes and frequency content expressed above.

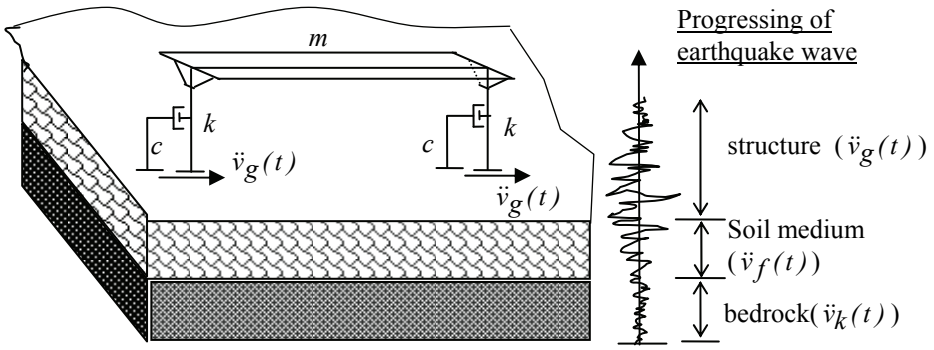

Figure 1. Progressing of earthquake motion from bedrock to structure

Table 1. Filter parameters

Parameter				
Soil type	ω_y (rad/s)	ξ_y	ω_d (rad/s)	ξ_d
hard	15.0	0.6	1.5	0.6
mild	10.0	0.4	1.0	0.6
soft	5.0	0.2	0.5	0.6

In stochastic analyses, nonstationary ground motions are usually represented by consideration of a random process having zero-mean Gaussian distribution multiplied with envelope functions for the amplitudes [19]. In this study, the process is defined to represent ground motion by white noise containing equally all frequency components and expressing uniform power spectrum intensity of S_o;

To reflect changes in the soil environment, stationary ground motions are taken into consideration in conjunction with filter functions. In this case, the power spectral density function of the process is defined by:

$$S_{\ddot{V}}(\varpi) = S_O \left|H_y(i\varpi)\right|^2 \left|H_d(i\varpi)\right|^2 \tag{1}$$

For this purpose, the filter of Kanai-Tajimi ($|H_y(i\varpi)|$) ampflying the high-frequency components near ϖ_y and damping rapidly the frequencies about $\varpi > \omega_y$ are used together with Penzien's filter function of $|H_d(i\varpi)|$ reducing rapidly the transition of low-frequency components ($\varpi < \omega_d$) as given in Eqs 2a and 2b [20]:

$$\left|H_y(i\varpi)\right|^2 = \frac{1+4\xi_y^2(\varpi/\omega_y)^2}{[1-(\varpi/\omega_y)^2]^2+4\xi_y^2(\varpi/\omega_y)^2} \tag{2a}$$

$$\left|H_d(i\varpi)\right|^2 = \frac{(\varpi/\omega_d)^4}{[1-(\varpi/\omega_d)^2]^2+4\xi_d^2(\varpi/\omega_d)^2} \tag{2b}$$

The soil dynamic characteristics of ξ_y, ω_y , ξ_d *and* ω_d refer the damping ratio and angular frequency for high and low frequency components, respectively. Values of these characteristics are given in Table 1 for three soil types [21]. Variations of the filter functions described by above functions are calculated for hard soil as illustrated in Figure 2.

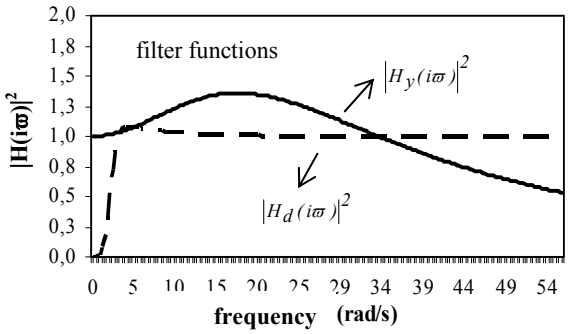

Figure 2. Filter functions for hard soil

2.2. Simulation of Nonstationary Earthquake Accelerations

In general, acceleration traces of a ground motion are expressed by time-varying function of *f(t)* as shown in Figure 3 [22]. This model is defined by three regions consisting of increasing amplitudes region, constant region and a decreasing region (in exponential form). The function parameters of t_1, t_2, t_3, t_4 and the exponential function constants μ *and* q are designated depending on duration of the earthquake record with strong ground motion (t_{eff}) and region's seismic properties. The parameters used in this study are specified by t_{eff} and time variations in amplitudes of the considered earthquake.

Power spectral density functions (PSDF) are computed for each soil group via Fourier transforms by using constant power spectral density of S_o. Through the relationship between mean square variations and PSDF, the amplitudes of ground motion *are obtained*

by seperating filtered power spectra $S_{\ddot{v}}(\varpi)$ into equal frequency intervals and by taking its integal:

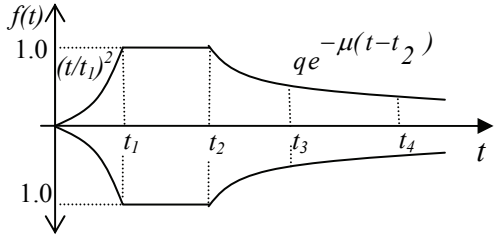

Figure 3. Time-varying envolope function

$$a_{xf}(t) = \sum_{k} \sqrt{4 S_{\ddot{v}}(k\Delta\varpi)\Delta\varpi}\cos(k\Delta\varpi t + \varphi_{kr}) \qquad r = 1,2,...N \quad k = 1,2,...N_S \tag{3a}$$

where φ_{kr} states phase angle between 0-2π interval of random process having uniform probability density function. N_s is the considered total number of equally spaced areas in the PSDF and N represents the number of generated random phase angles for the r [nd] sample function. Generated stationary amplitudes are handled together with the envelope function of f(t) given in Figure 3:

$$\ddot{v}_g(t) = f(t).\, a_{xf}(t) \tag{3b}$$

In this study, aritificial ground motions are desired to obtain in accordance with the frequency content and the amplitude variations of the Erzincan 1992 earthquake NS record by the approach of harmonic model given above. For this purpose, the amplitudes are derived by Eq.3 via Kanai-Tajimi spectrum (Eq. 2) and filter functions based on dynamic characteristics of the ground given in Table 1. For time-varying function f(t), since the parameters calculated by the values given in literature yielded unsuitable ground motions according to recorded motion, compatiple values of the parameters are probed. Therefore, artificial ground motions are simulated by sequential approaches and regression analyses which are implemented to resolve incompatibility and to achive optimum values of the parameters. Constant power spectral intensities are calculated as 52,9, 74,4 ve 108,0 cm^2/s^3 for hard, mild and soft soil, respectively [23]. The PSDF of Erzincan 1992 earthquake and filtered power spectra for soil types are shown in Figure 4 and 5. Through the obtained power spectra, 20 artificial acceleration records are simulated for each of 4 different soil types and samples of those simulated ones are shown in Figure 6.

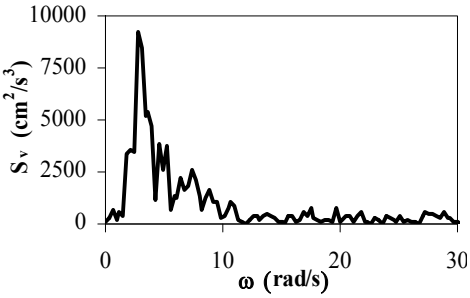

Figure 4. Power spectrum-Erzincan NS 1992

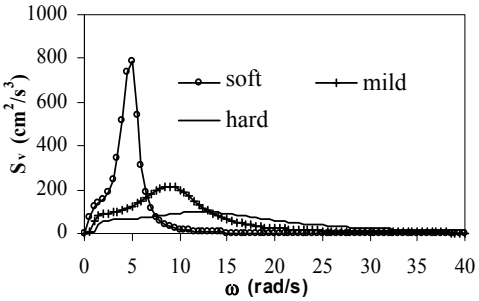

Figure 5. Filtered power spectra for soil types

The power spectra obtained for the soil types are drawn by dotted lines as shown in Figure 7 on the basis of averaging the values of the power spectrum corresponding to artificial acceleration records. Smoothed process is executed over the curves for a better understanding of the spectrum and providing ease in comparison and the resulting curves are drawn by a solid line (Figure 7).

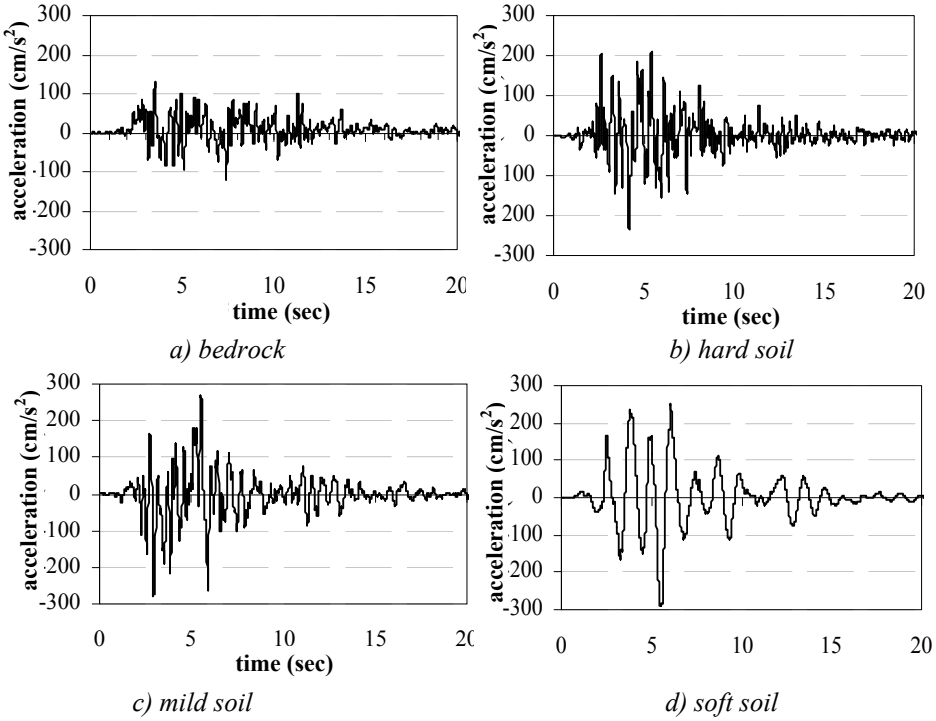

Figure 6. Examples of acceleration records from artificial earthquake motions

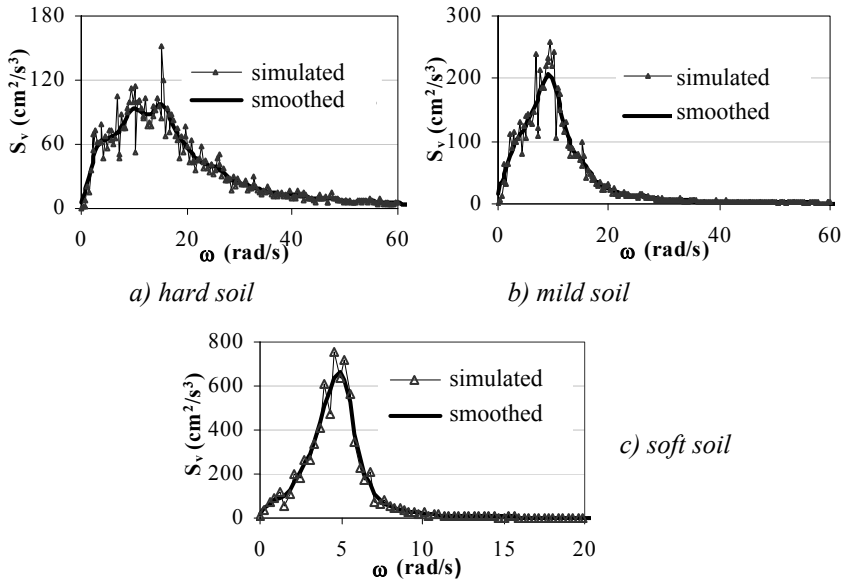

Figure 7. Smoothing process for power spectra

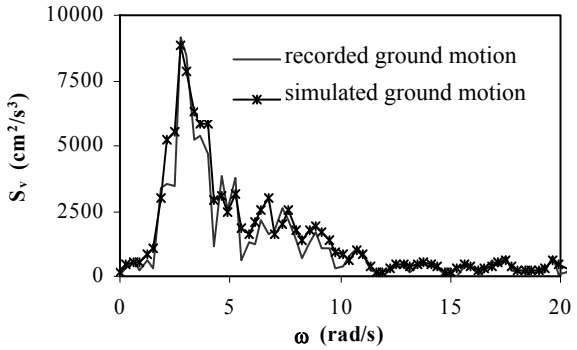

Figure 8. Comparions of the power spectra

In Figure 8, the average power spectrum, calculated from artificial accelerations generated by the envelope function using the appropriate parameter values, is compared with that of Erzincan NS 1992 component. As seen from the figure, it is understood that the derived power spectrum is to be consistent with the current motion and artificial records reflect the power of the recorded motion. Similarly, consistency of the artifical motions is checked out by a comparison given in Figure 9 in terms of distribution of frequency content and variances. From the comparisons, it is drawn that artificial ground motions can represent

recorded ground motion characteristics in terms of frequency and amplitude variations as well.

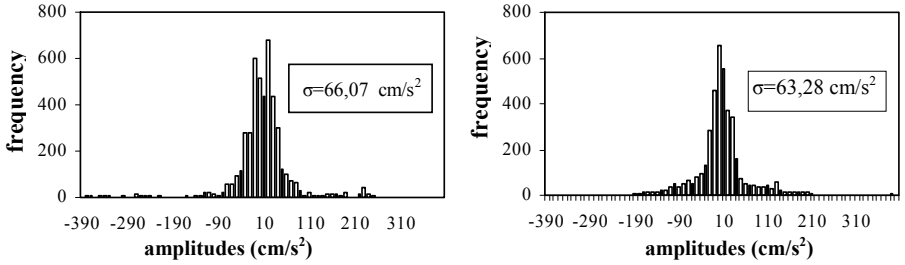

a) recorded ground motion *b) artificial ground motion*

Figure 9. Frequency distributions for recorded and artificial motions

3. PIER SYSTEM AND STOCHASTIC BEHAVIOR

Reinforced bridge pier with variable cross-section of V-beam of the support and also consisting of rectangular box section of pier column is considered as shown in Figure 10. Two lead core rubber bearings are seated under the deck-beam in each end edge. For pier system linear elastic behavior and for rubber bearings both non-linear and linear behavior has been seperately taken into consideration. For the pier system, analyses are carried out by 5% damping ratio.

3.1. Defining of Pier Model and Free Vibration Analysis

The pier system is modeled with a prismatic frame type finite element assigned between the nodes located with different mesh intervals in horizontal and vertical directions. A system having 12 degree of freedoms (DOF) is defined instead of a second system with 21 DOF to decrease the computations of stochastic dynamic analysis. The finite element models created for the pier system under efffects of lateral ($a_x(t)$) and vertical ($a_y(t)$) accelerations are shown in Figure 10 with the freedoms and consideration of the lumped mass on the nodes. By forming system stiffness matrix, dynamic stiffness matrix corresponding to the vibration of freedoms is obtained by static condensation. In the solutions, linear analysis is performed in the first stage for the entire system by considering the rubber bearing's horizontal (R_x), vertical (R_v) and rotational stiffnesses as (R_ϑ).

Nonlinear bahavior (Figure 11) of the lead core rubber isolator (with steel plates) modeled by spring elements is discussed in the analysis for comparison purposes. The characteristic stiffness of the isolator is calculated with the formula given in the literature ([24], [25], [26]). The effective stiffness (K_{eff}) charaterizing cycle behavior, is expressed by sum of the ratio of characteristic strength ($Q < F_y$) to displacement capacity (δ) and post-elastic rigidity (K_d):

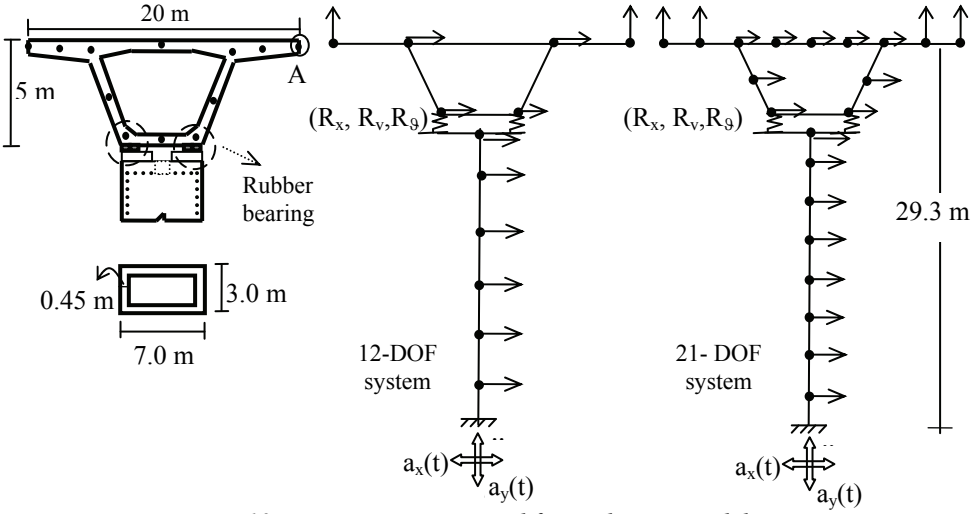

Figure 10. Pier cross-section and finite element models

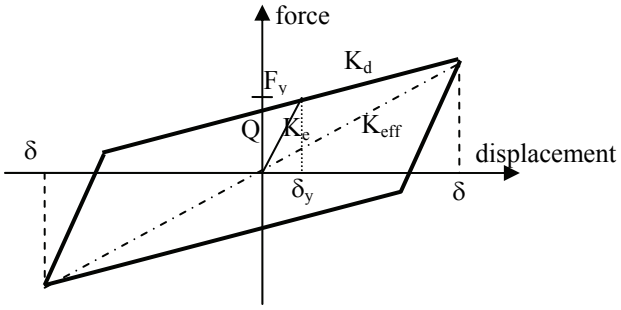

Figure 11. Rubber isolator behavior model

$$K_{eff}=K_d+Q/\delta \quad (\delta>\delta_y) \quad (Q < F_y) \tag{4}$$

The ratio of the post-yield stiffness (K_d) to the elastic stiffness (K_e) is presumed as 0.133 and shear modulus (G) of the rubber material is considered as 1 N/mm^2. The effective damping ratio $\bar{\beta}$ is computed as 0.128 by the relation given in Eq. 5 based on cyclical behavior area of rubber bearing ($4Q(\delta-\delta_y)$), effective stiffness and displacement values:

$$\bar{\beta}=\frac{2Q(\delta-\delta_y)}{\pi\delta^2 K_{eff}} \tag{5}$$

Stochastic dynamic analyses of the pier system are carried out by a developed algorithm and time domain analyses by software package SAP2000 [27]. The pier mode shapes obtained from the free vibration analysis are shown in Figure 12. The accuracy of the reduced degree of freedoms sytem from 21 DOF to 12 DOF is provided in sufficient level by the comparisons (Table 2) of periods and effective modal mass contributions. As it is well known, horizontal stiffness of the rubber isolator is quite low as compared to that of vertical and this property provides large flexilibity to structural system. Therefore, the first mode shape has occured in lateral direction as expected. The isolator period calculated by $T_{iz} = 2\pi\sqrt{W/K_{eff}g}$, is obtained as T_{iz}=1.76 sec to be close to the first period (T_1=1,82 sec) of the pier system where effective stiffness is K_{eff}, total structure weight W and acceleration due to gravitiy is g.

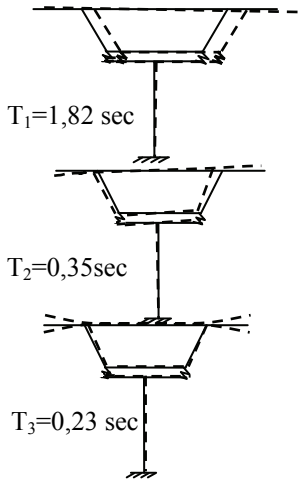

Table 2. Periods and modal mass contribution

Mode no	T-(s) (12-DOF)	T-(s) (21-DOF)	Effective mass (12-DOF)	Effective mass (21-DOF)
1	1.82	1.82	0.8192	0.8202
2	0.47	0.35	0.8199	0.8202
3	0.34	0.23	0.8199	0.8202
4	0.15	0.13	0.8250	0.8519
5	0.12	0.12	0.9431	0.9390

Figure 12. Free vibration mode shapes (21 DOF)

As it is known, the isolator period is generally larger than the structure period. Although an isolator period is based on the principal of choice of the the isolator characteristics, it has developed close to the first period of the system in this example.

3.2. Stationary Stochastic Model

Under the effects of earthquake loads, power spectra are derived to define random input process (p(t)) and output process (v(t)) which is obtained by means of transfer functions (TF) where the pier system remained completely in the linear elastic behavior range. Since randomness in the transfer functions is much lower compared to that of ground motion, the adoption for TF_1=TF_2, .., TF_N=TF is considered as a single function in the computations. General equation of motion (defining dynamic behavior) of a multi-DOF system under effect of ground motion effects $\ddot{v}_g(t)$,

$$[m]\{\ddot{v}(t)\}+[c]\{\dot{v}(t)\}+[k]\{v(t)\}=\{p(t)\}=\{-m.\ddot{v}_g(t)\} \tag{6}$$

where ***[m]*** is the mass matrix, ***[c]*** is the damping matrix, ***[k]*** is the system stiffness matrix and vector of ***{v}*** express the relative displacements. In linear solutions, load effects ***{p(t)}*** are able to be decomposed into harmonic components by Fourier transformations. If inverse Fourier transforms are realized over the harmonic components defined in frequency domain, the behavior is obtained by the following relation,

$$v(t)=\frac{1}{2\pi}\int_{-\infty}^{\infty} H(i\varpi)Z(i\varpi)e^{i\varpi t}d\varpi \tag{7}$$

where $H(i\varpi)$ states complex frequency response function and $Z(i\varpi)$ is the Fourier transformation of force function. The frequency response function is

$$H(i\varpi)=\frac{1}{k[1+2i\xi(\varpi/\omega)-(\varpi/\omega)^2]} \tag{8}$$

defined by the given relation. In obtaning generalized modal forces, modal responses are identified by cross-power spectral density function (Sp_mSp_n) defined for discrete modes of n, m and by superpositon of frequency response functions. Thereby, variances are obtained by square variations in PSDF of any response point as follows

$$\sigma_v^2(t)=\sum_m\sum_n B_mB_nS_{P_mP_n}\int_{-\infty}^{+\infty} H_m(i\varpi)H_n(-i\varpi)d\varpi \tag{9}$$

where B_n ve B_m are the coeefficients that can be found by standard structural solution techniques. When the modes are sufficiently seperated meaning to be statistically independent from each other, and if Eq. 9 is written also the for the same modes,

$$\sigma_v^2(t)=\sum_m B_m^2S_{p_mp_m}\int_{-\infty}^{+\infty}\left|H_m(i\varpi)\right|^2 d(\varpi) \qquad m=1,2,.....,N \tag{10}$$

the responses neglecting the contribution of cross-terms are achieved. This function indicates the relationship between output and input in the system by numerical quantities. The frequency response function in case of statistical independence is defined by,

$$\left|H_m(i\varpi)\right|^2==\frac{1}{K_m^2[1+(4\xi_m^2-2)(\varpi/\omega_m)^2+(\varpi/\omega_m)^4]} \tag{11}$$

where K_m is the generalized stiffness. If the modes are dependent, integration of the frequency response function can not be easily realized by conventional methods due to existing complex variables. In order to overcome this difficulty, Residue method is

implemented for numerical calculations. In order to express the effects (p_{eff}) of ground motion in the horizontal and vertical directions, generalized force function

$$P_n(t)P_m(t) = \{\phi_n^T\}[m]\begin{Bmatrix} a_y(t) \\ a_y(t) \\ \vdots \\ \vdots \\ a_x(t) \end{Bmatrix}[a_y(t)\, a_y(t)\cdots a_x(t)][m]\{\phi_n\} \tag{12}$$

is defined by two-discrete modes. If the power intensity of the horizontal earthquake component is selected as a stationary process model of $S_{\ddot{u}_x\ddot{u}_x} = S_o$, the intensities in the other directions may be expressed by correlation coefficients such as $S_{\ddot{u}_y\ddot{u}_y} = \alpha S_o$ and $S_{\ddot{u}_x\ddot{u}_y} = S_{\ddot{u}_y\ddot{u}_x} = \beta S_o$. In this case cross-power spectral density of the discrete force function is defined by,

$$S_{P_mP_n}(\varpi) = \{\phi_m^T\}[m]\, S_o \begin{bmatrix} [\alpha]_{d\times d} & [\beta]_{d\times y} \\ [\beta]_{y\times d} & [1,0]_{y\times y} \end{bmatrix}_{N\times N} [m]\{\phi_n\} \quad m=1,2,...,N \quad n=1,2,...,N \tag{13}$$

where d is the number of vertical freedoms and y is the number of horizontal freedoms. The values of α and β correlation coefficients are taken as 0.444 and 0.67, respectively depending on the power of the considered earthquake spectrum. If the force vector is expressed by generalized displacement $Y_n(t)$, moment (M_n) and shear force (V_n) at any point can be calculated with the formula given below:

$$M_n(t) = \sum_{n=1}^{N} B_n\omega_n{}^2[m]\{\phi_n\}Y_n(t) \qquad V_n(t) = \sum_{n=1}^{N} A_n\omega_n{}^2[m]\{\phi_n\}Y_n(t) \tag{14}$$

where N is the total number of degree of freedoms. The coefficients A_n and B_n in equation 14 are determined by standard structural analysis.

4. TIME HISTORY ANALYSIS AND RESPONSE FACTORS

Peak response factors of the pier system exposed to nonstationary ground effects are derived depending on different conditions of rubber bearing and various soil types. The peak response factors of the base reactions (V, M) and deck displacements (D) are obtained as shown in Figure 13 for different soil types. The variations in peak factors are illustrated for supporting types (rigid and rubber bearing) of superstructure and nonlinear behavior of the rubber bearing system. Instead of using the rubber bearing supporting the deck system, in case of use of rigid connections the peak factors reach highest values (4-4.5).

Rubber bearings providing flexibility to the system allow for the lowest values (2.88-3.4) of peak factors. Both nonstationary features and different power intensities of the soil sites affect the response quantities and cause to appear in a range of peak factors. In a study of suspension bridge subjected to stationary motions, Datta [14] has achieved the peak factors in the range of 2.81- 3.22. Nonlinear behavior of the rubber material is observed to increase significantly these factors as seen from the figures. The reason of the larger peak factors in the non-linear behavior is the increments of the variances of structural response. It is clearly understood that these responses have low peak factors in case of linear behavior. Variances of the base shear force are shown in Figure 13d together with increment ratios of the responses for soil types by normalized according to the results of bedrock ground motion's variances.

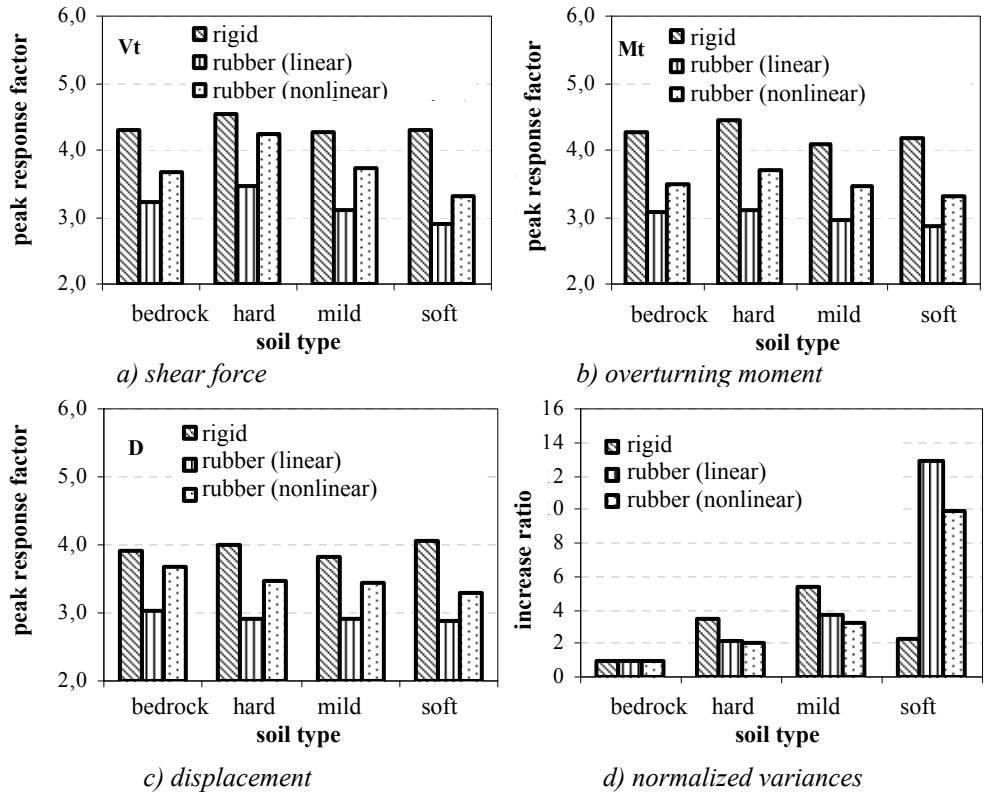

Figure 13. Peak response factors and normalized variances

For the isolated system, increment ratio in the variances of base shear force (V), overturning moment (M) and the horizontal displacement (D) is around 1.5 times while transition from the type of hard soil to mild soil, but calculated increment becomes about 5-6 times for the soft soil type. As expected, the largest increase rates appear in rigid case

(connection) but the results diverge in case of soft soil and nominal quantities in the response therefore variances started to sharply decline. The soft soil condition lead to significant changes for all cases in structural behavior and it caused to develop large variance values especially by influencing negatively the behavior of the isolated system.

5. COMPARISONS OF FREQUENCY AND TIME DOMAIN SOLUTIONS

The reactions in bridge pier are obtained depending on the structural characteristics, the fairly conformable modal responses and the generated earthquake records derived in the previous section by the analyses realized in the time and frequency domain. Peak responses in the pier system are determined in terms of different ground conditions and supporting cases under effects of horizontal component of the ground motion and simultaneously with its 2/3 times amplitudes in the vertical direction. In statistical expressing of expected peak responses, three cases are taken into consideration: linear behavior, nonlinear behavior of rubber bearing and rigid connection without rubber bearings. For the maximum base responses, the mean values calculated in the frequency domain by stochastic method are compared by those of the time domain solutions for each soil type.

When the peak base responses (in frequency domain) of the isolated pier system are compared with the solutions in the time domain (Figure 14), it is observed that the stochastic method generally yields quite consistent results. However, significant differences are determined in base responses especially for the bending moment in case of soft soil case. When the isolated pier system is modelled with 21 DOF by discretized smaller mesh intervals, the peak values obtained for the responses are shown in Figure 14c and 14d. As the results are compared with Figure 14a and 14b, although closer results partially for shear forces are obtain by increasing the number of DOF, there are no significant changes in the moment values. From plotted graphics, dynamic solutions of the finite element model defined by 12 DOF are understood to be enough.

As it is generally expected, in the case of rigid connection of the pier that response values for hard and mild soil types increase rapidly but a decrement is observed for soft soil. In general, the solutions in frequency domain has yielded lower response values compared to the time domain solutions except for the soft soil set (Figure 14 e,f). While it seems to be an increment in the responses of soft soil for the time domain solutions, a decrease occur in the frequency domain solutions. General solutions computed for earthquake ground motions with the amplitudes nonstationary in the frequency domain are also attempted to obtain from the time domain solutions by using simulated ground motions based on the spectral power of the same earthquake. Therefore, in developing consistent results are expected in this regard by applying the two different approaches. Some studies in the literature may provide more consistent results for stationary ground motions [14].

Responses in time domain obtained by nonlinear rubber behavior are compared with those of the linear frequency domain based on equivalent linear stiffness and the results are illustrated in Figure 15. The differences observed in the results of the both solution methods are pointed as; while the system responses considered with nonliner behavior of rubber bearing take too low values for bedrock, they show significant differences in other soil types especially for base shear force V(t).

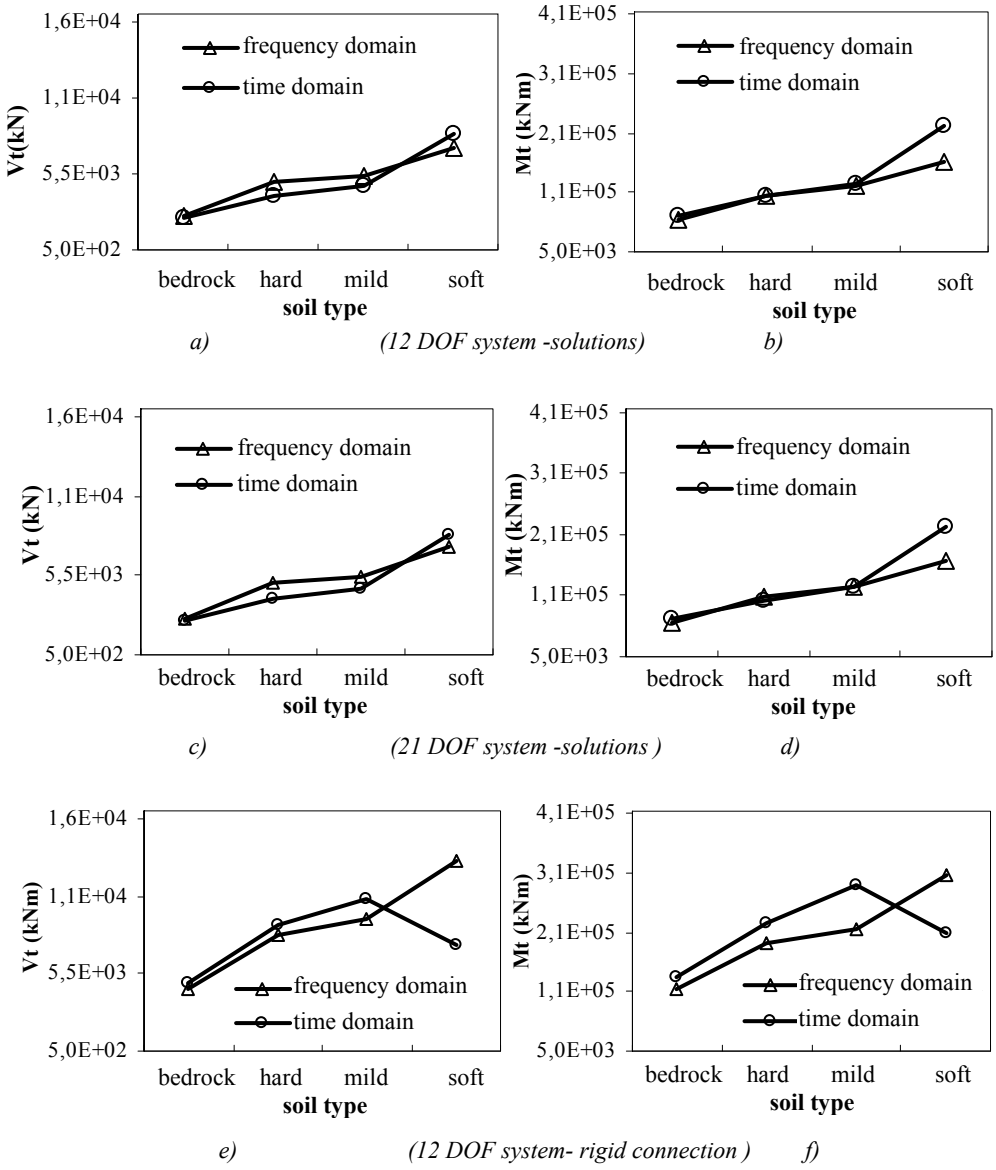

Figure 14. Comparisons of expected mean values of the base peak responses depending on the soil types

The main reason of the general differences in both solutions might be mentioned that stochastic solutions are directly obtained in the way of general solutions through PSDF. Under seismic effects taken into consideration, the superiority of the stochastic method should be noted in the expression of responses by statistical terms for the linear analysis. In

order to obtain statistical response values; while great numbers of artificial earthquake records are needed for each soil type in time history domain analyses taking long time, stochastic methods directly yield statistical results by a single frequency domain solution for a soil type considered.

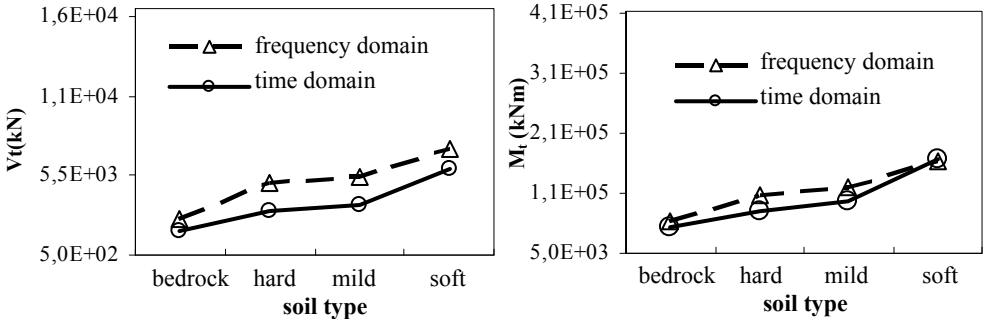

Figure 15. Nonlinear analysis in time domain and frequency domain analysis with linear behavior

6. PROBABILITY DISTRIBUTIONS FOR PEAK RESPONSES

In earthquake-resistant design, identification of an acceptable risk or exceedance probability during life of structure plays an important role in the design philosophy (or codes) for the considered demands stemming from strong accelerations. Structural safety is expressed by an exceedance probability of a prescribed design or reference value by modelling the nonstationary peak responses (given in section 5) based on a probability distribution. For this purpose, a random variable X representing the maximum response at any point in the structure is defined by an assumption of asimptotic distribution function fitting to Rayleigh distribution,

$$f(x) = \frac{x}{\alpha_r^2} exp[-\frac{1}{2}(\frac{x}{\alpha_r})^2] \qquad x \geq 0 \tag{15}$$

where α_r is the scale parameter of distribution which is determined based on the avaliable data. Since twenty solutions are executed for each soil type, the parameters of the Rayleigh distribution are estimated by using the results obtained from the analyses of the each sample. Mean value ($\overline{x}$), standard deviation (σ_x) and dispersion parameter (α_r) are shown for deck peak horizontal displacements on edge ends (Figure 10, A-point) in Table 3.

Table 3. Rayleigh distribution parameters of deck displacements

Soil type	$\overline{\mathbf{x}}$ (m)	$\boldsymbol{\sigma_x}$ (m)	$\boldsymbol{\alpha_r}$
hard	0.147	0.044	0.108
mild	0.191	0.057	0.141
soft	0.351	0.108	0.259

Probability density and exceedance probability functions obtained for peak displacements are plotted in Figure 16 depending on soil type. The shape of distribution functions are very similar for the hard and mild soil because of closeness of their standard deviation values, whereas a wider scattering is observed for soft soil type. While the peak displacements take close values in high-exceedance probabilities for all soil types, the responses of soft ground case clearly dissociate itself from the other soil types under the 75 % exceding risk level.

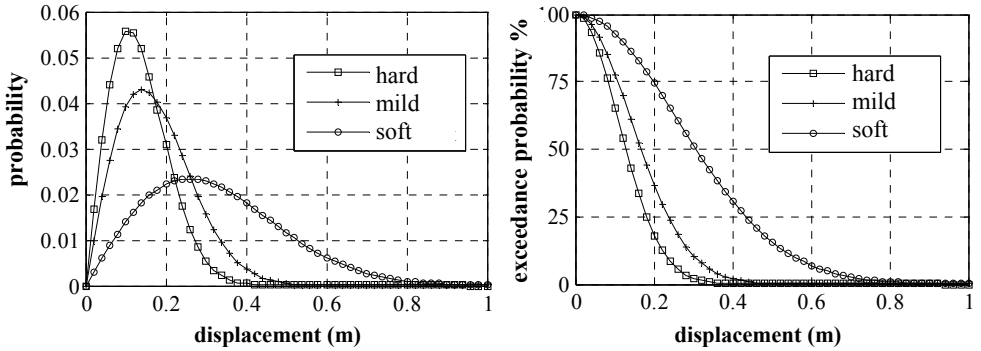

a) probability density functions *b) exceedance probability functions*

Figure 16. Probability functions for deck displacements

The expected peak values of deck displacements are calculated with regard to exceedance probability levels with soil types and shown in Table 4. Furthermore, the exceedance probability functions obtained from the base responses (shear forces (V) and overturning moments (M)) are shown in Figure 17.

Table 4. Peak displacements (m)

soil type	exceedance level		
	2%	**10%**	**50%**
hard	0.302	0.232	0.127
mild	0.394	0.303	0.166
soft	0.726	0.557	0.305

As seen from the tables and graphs, response values of soft soil condition are rapidly observed to increase in exponential form by decreasing exceedance probabilities.

The peak responses are estimated by exceedance probability functions and shown for some exceedance levels in Table 5. In order to obtain a dimensionless quantity, peak displacements and base response values are normalized by the mean values to investigate increases in responses for different exceedance levels. Structural responses normalized by the values of D, V, and M corresponding to exceedance probability of 50% are shown in

Table 6. Increase ratios in responses for the exceedance probabilities of 10% and 2% are obtained as 1.82 and 2.38 times, respectively for all soil conditions.

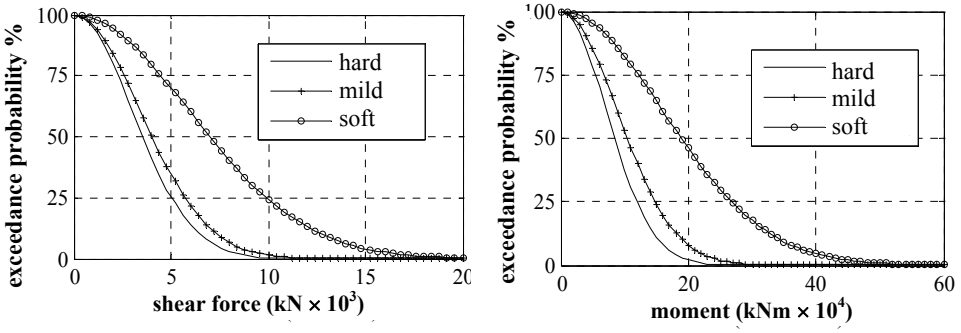

Figure 17. Exceedance probability functions for base responses

Table 5. Peak base responses

Soil type	V (kN)			M (kNm)		
	2%	10%	50%	2%	10%	50%
hard	8447	6481	3556	200241	153624	84288
mild	9584	7353	4034	247765	190085	104292
soft	16629	12760	6999	448855	344361	188938

Table 6. Normalized peak ratios by mean

Soil type	D, V, M		
	2%	10%	50%
hard	2.375	1.823	1.000
mild	2.376	1.823	1.000
soft	2.376	1.823	1.000

Physical safety might be expressed such as reliability index or level of risk through probabilistic values and exceedance / probability distribution functions obtained for peak responses. Peak response quantities obtained for a given probability level that can be used in the design may make sense of increment increase ratios for soil types and exceedance probability functions in the evaluation of such pier systems. However, a parametric study containing numerous analyses is needed to derive a general inference for the design of existing different systems or newly to be constructed piers.

7. DISCUSSIONS

- In this study, the influences of different soil sites and supporting conditions of rubber bearing are investigated for a specific example given the properties of geometry and rigidity of a constructed bridge pier. For this purpose, peak responses, probability-based response quantities (cross-section reactions, displacements) and exceedance / probability distribution functions are calculated by means of simulated ground motions.
- Under nonstationary earthquake effects, peak response factors (r) are computed in the range of 2.88-4.5 depending on soil types and three different supporting conditions of deck. These factors exhibit even a little upward trend with increasing of the soil rigidity. Linear behavior of the rubber bearings has enabled to take the lowest values (2.88 to 3.4) of these factors. However, the nonlinear behavior of rubber bearing cause significant increases in the factors. In case of rigid connection, these factors reach the largest values (4-4.5). In Vanmarcke model, peak response factors are approximately computed as 3.45 for each soil type by considering earthquake duration of t_d=20 sec used in this study and reliability level of 95%
- Soft soil condition leads to great alteration of the variances with large increment of the peak ratios by negatively affecting the isolated system. Therefore, it should be avoided from the interactions between the soil dominant period and the structural system period in the design of an isolated bridge system. A trend in the opposite direction is seen for the soft soil site in the rigid connection case and the variance increment ratios drop significantly.
- In this special example it is observed that the responses obtained in the frequency domain are comparable with the time domain solutions and the stochastic method represented for the randomness of the frequency content has yielded accurate results especially for linear analysis of the pier system having rubber bearings. It is naturally expected once nonlinear behavior of rubber bearing considered that the frequency domain would yield great response values according to solutions in the time domain and therefore different results are obtained.
- The less compuation effort for obtaining the statistical quantities of the responses through direct PSDF shows the superiority of the stochastic method for elastic solutions in practice. However, simulating a large number of ground motions and structural analyses are needed in the time domain to express the responses by statistics.
- For the peak responses dealt with Rayleigh distribution, although the probability density and exceedance probability functions are observed to be close to each other for hard and mild soil sites, a broader scattering are observed in case of soft soil even for low exceedance probabilities with significantly increasing base reactions and displacements.
- In non-damaged elastic behavior of the bridge pier under earthquake effects, the normalized peak responses obtained herein as a property of Rayleigh distribution for base shear forces, overturning moments and deck displacements become independent from the soil types but depend on levels of exceedance probability.

- When the peak responses normalized by the value of exceedance probability of 50% are evaluated by probability of exceedance levels of 10% and 2%, increase in responses become 1.82 and 2.38 times, respectively and these increment ratios are the same for all ground conditions. Under favour of this feature, the peak responses of other soil types can be directly calculated without performing analyses by using the obtained increment ratios with reference to a soil type and mean value of the considered soil type.
- Advanced probabilistic analyses such as structural reliability or risk analysis can be performed by the obtained exceedance/probability distribution functions and through statistical characteristics of the responses. Furthermore, the peak responses of the considered pier system that is usable in designs can be directly calculated by using obtained peak factors. However, parametric studies are required to derive a general inference for different bridges and pier systems.

Symbols

A_n, A_m	: moment coefficients for n^{th} and m^{th} modes
$a_x(t)$, $a_y(t)$	: horizontal and vertical accelerations
$a_{xf}(t)$	: filtered acceleration record
B_n, B_m	: shear force coefficients for n^{th} and m^{th} modes
$[E(x_{max})]$	: expected mean of the peak values
f(t)	: envolope function
f(x)	: Rayleigh distribution function
G	: shear modulus
PSDF	: power spectral density function
$\|H_y(i\varpi)\|$, $\|H_d(i\varpi)\|$	: filter functions for high and low frequency components
$H(i\varpi)$	: frequency response function
RMS	: Root mean square value
K_{eff}, K_d	: effective and post-yield stiffness of rubber bearing
K_m	: generalized stiffness
M_n, V_n	: n^{th} modal moment and shear force at the pier base
N_s, N	: number of equally spaced areas and phase angle
[m], [c], [k]	: mass, damping and stiffness matrix
Q, F_y	: characteristic and yield strength
p(t), v(t)	: input and output process
{p(t)}	: load vector
p_{eff}	: effective force of ground motion
$P_n(t)$, $P_m(t)$	: generalized n^{th} and m^{th} forcing function

q	: constant for exponential function
r	: peak response factor
R_x, R_v, R_ϑ	: horizontal, vertical and rotational stiffness of rubber bearing
S_o	: constant power spectral intensity
Sp_mSp_n	: cross-power spectral density function
$S_{\ddot{u}_x\ddot{u}_x}$, $S_{\ddot{u}_y\ddot{u}_y}$	: power spectrum intensities in lateral and vertical directions
$S_{\ddot{u}_x\ddot{u}_y}$, $S_{\ddot{u}_y\ddot{u}_x}$	: cross-power spectrum intensities
$S_{\ddot{v}}(\varpi)$	: power spectral density function
t_1, t_2, t_3, t_4	: parameters of envolope function
t_{eff}	: effective duration of strong ground motion
T, T_{iz}	: periods for pier system and isolator
TF_i	: transfer function
{v}	: relative displacement vector
$\ddot{v}_k(t), \ddot{v}_f(t), \ddot{v}_g(t)$	: acceleration in bedrock, soil medium and ground surface
$\overline{x}$	: mean value
$Y_n(t)$	: generalized modal displacement
$Z(i\varpi)$	: Fourier transformation of forcing function
α, β	: corelation coffeecients for power intensity
α_r	: Rayleigh distribution parameter
$\overline{\beta}$	: effective critical damping ratio
$\Delta\varpi$	: frequency intervals
ξ_y, ξd	: damping ratios for high and low frequency components
φ_{kr}	: phase angle
$\{\phi\}$	: modal vector
δ, δ_y	: displacement capacity and yielding displacement
μ	: constant for exponential function
ω_y, ω_d	: angular frequencies for high and low frequency components
$\ddot{v}_g(t)$	: amplitudes for nonstationary acceleration
σ_v, σ_x	: standard deviations

Acknowledgement

Authors thank Dr. Barış Erkuş who read the article and shared his valuable evaluations.

References

[1] Jia, H. Y., Zhang, D. Y., Zheng, S. X., Xie, W. C., Pandey, M. D., Local Site Effects On a High-Pier Railway Bridge under Tridirectional Spatial Excitations: Nonstationary Stochastic Analysis, Soil Dynamics and Earthquake Engineering 52, 55–69, 2013.

[2] Li, Y., Chen N., Zhao, K., Liao, H., Seismic Response Analysis of Road Vehicle-Bridge System for Continuous Rigid Frame Bridges with High Piers, Earthquake Engineering and Structural Dynamics, 11, 593-602, 2012.

[3] Mahmoud, S., Austrell, P. E., Jankowski, R., Simulation of the Response of Base-Isolated Buildings under Earthquake Excitations Considering Soil Flexibility, Earthquake Engineering & Engineering Vibration, 11(3), 359-374, 2012.

[4] Dicleli, M., Karalar, M., Optimum Characteristic Properties of Isolators with Bilinear Force–Displacement Hysteresis for Seismic Protection of Bridges Built on Various Site Soils, Soil Dynamics and Earthquake Engineering 31, 982–995, 2011.

[5] Ala Saadeghvaziri, M., Foutch, D. A., Dynamic Behavior of RC Highway Bridges under the Combined Effect of Vertical and Horizontal Earthquake Motions, Earthquake Engineering and Structural Dynamics, 20(6), 535-549, 1991.

[6] Ala Saadeghvaziri, M., Foutch, D. A., Foutch, Behavior of RC Columns under Non-proportionally Varying Axial Load, Journal of Structural Engineering, 116(7), 1835-1856, 1990.

[7] Pagnini, L. C., Solari, G., Stochastic Analysis of the Linear Equivalent Response of Bridge Piers with Aseismic Devices, Earthquake Engineering and Structural Dynamics, 28, 543-560, 1999.

[8] Jangid, R. S., Equivalent Linear Stochastic Seismic Response of Isolated Bridges,Journal of Sound and Vibration, 309, 805-822, 2008.

[9] Kunde, M. C., Jangid, R. S., Effects of Pier and Deck Flexibility on the Seismic Response of Isolated Bridges, Journal of Bridge Engineering, 11(1), 109-121, 2006.

[10] Gongkang, F., Elastically Supported Cantilever Beam Subjected to Nonstationary Seismic Excitation, Earthquake Engineering and Structural Dynamics, 27, 977-995, 1998.

[11] Hasgür, Z., Stochastic Analysis of Bridge Piers with Symmetric Cantilevers under the Base Accelerations, Bulletin of the Istanbul Technical University, 48(3-4) 657-667, 1995.

[12] Ates, S., Bayraktar, A., Dumaoglu, A. A., The Effect of Spatially Varying Earthquake Ground Motions on the Stochastic Response of Bridges Isolated with Friction Pendulum Systems, Soil Dynamics and Earthquake Engineering, 26, 31-44, 2006.

[13] Sungur, I., Stochastic Response to Earthquake Forces of a Cable-Stayed Bridge, Engineering Structure, 15(5), 307-314, 1993.

[14] Allam, Said M. Datta, T. K., Response Spectrum Analysis of Suspension Bridges for Random Ground Motion, Journal of Bridge Engineering, 7(6), 325-337, 2002.

[15] Zhang, Z. C., Lin, J. H., Zhang, Y. H., Zhaoa, Y., Howsonc, W. P., Williams, F. W., Non-Stationary Random Vibration Analysis for Train–Bridge Systems Subjected to Horizontal Earthquakes, Engineering Structures 32, 3571–3582, 2010.

[16] Vanmarcke, E. H., Lomnitz, C., Rosenbleuth, E., Structural Response to Earthquakes, Chapter 8 in Seismic Risk and Engineering Decisions, Elsevier, New York, 1976.

[17] Davenport, A. G., Note on the Distribution of Largest Values of Random Function with Application to Gust Loading, Proc. Inst. of Civil Eng., 28, 187–196, 1964.

[18] Mylonakis, G., Syngros, C., Gazetas, G., Tazoh, T., The Role of Soil in the Collapse of Piers of Hanshin Expressway in the Kobe Earthquake, Earthquake Engineering and Structural Dynamics, 35, 547-575, 2006.

[19] Jangid, R. S., Equivalent Linear Stochastic Seismic Response of Isolated Bridges, Journal of Sound and Vibration, 309, 805-822, 2006.

[20] Clough R. W., Penzien, J., Dynamics of Structures, Mc-Graw Hill Book Company, Second Edition, New York, 1993.

[21] Der Kiureghian, A., Neuenhofer, A., A Response Spectrum Method for Multiple-Support Seismic Excitations, UCB/EERC-91/08, University of California, Berkeley, 1991.

[22] Jennings, P.C., Housner, G. W., Tsai, N. C., Simulated Earthquake Motions for Design Purposes, Proc. 4th World Conf. Earthquake Engineering, 1(a-1), 145–160, Chile, 1969.

[23] Sarıtaş, F., Stochastic Dynamic Analysis of Box-Girder Bridges, Phd Dissertation, Istanbul Technical University, 2007.

[24] Naeim, F., Kelly, J. M., Design of Seismic Isolated Structures, John Wiley & Sons, Inc., U.S.A., 1999.

[25] AASHTO, AASHTO LFRD Bridge Design Specifications, American Association of State Highway and Transportation Officials, Joints and Bearings, Washington D.C, 2007.

[26] DIN 4141-14, Structural Bearings, Laminated Elastomeric Bearings Design and Construction, Deutsche Institut für Normung, 1985.

[27] SAP2000, Structural Analysis Program, Computers and Structures Inc., Berkeley, 1995.